

Human Molecular Genetics

Premature aging in mice activates a systemic metabolic response involving autophagy induction

Guillermo Mariño, Alejandro P. Ugalde, Natalia Salvador-Montoliu, Ignacio Varela, Pedro M. Quirós, Juan Cadiñanos, Ingrid van der Pluijm, José M.P. Freije and Carlos López-Otín

Hum. Mol. Genet. 17:2196-2211, 2008. First published 28 Apr 2008;

doi:10.1093/hmg/ddn120

Supplement/Special IssueThis article is part of the following issue: "*Supplementary Data*"
<http://hmg.oxfordjournals.org/cgi/content/full/ddn120/DC1>The full text of this article, along with updated information and services is available online at
<http://hmg.oxfordjournals.org/cgi/content/full/17/14/2196>**References**This article cites 76 references, 24 of which can be accessed free at
<http://hmg.oxfordjournals.org/cgi/content/full/17/14/2196#BIBL>**Supplementary material**Data supplements for this article are available at
<http://hmg.oxfordjournals.org/cgi/content/full/ddn120/DC1>**Reprints**Reprints of this article can be ordered at
http://www.oxfordjournals.org/corporate_services/reprints.html**Email and RSS alerting**Sign up for email alerts, and subscribe to this journal's RSS feeds at <http://hmg.oxfordjournals.org>**PowerPoint®
image downloads**

Images from this journal can be downloaded with one click as a PowerPoint slide.

Journal informationAdditional information about Human Molecular Genetics, including how to subscribe can be found at <http://hmg.oxfordjournals.org>**Published on behalf of**Oxford University Press
<http://www.oxfordjournals.org>

Premature aging in mice activates a systemic metabolic response involving autophagy induction

Guillermo Mariño¹, Alejandro P. Ugalde¹, Natalia Salvador-Montoliu¹, Ignacio Varela¹, Pedro M. Quirós¹, Juan Cadiñanos¹, Ingrid van der Pluijm², José M.P. Freije¹ and Carlos López-Otín^{1,*}

¹Departamento de Bioquímica y Biología Molecular, Facultad de Medicina, Instituto Universitario de Oncología, Universidad de Oviedo, 33006 Oviedo, Spain and ²DNage, Department of Genetics, Erasmus University Medical Center, Rotterdam, The Netherlands

Received February 1, 2008; Revised March 18, 2008; Accepted April 9, 2008

Autophagy is a highly regulated intracellular process involved in the turnover of most cellular constituents and in the maintenance of cellular homeostasis. It is well-established that the basal autophagic activity of living cells decreases with age, thus contributing to the accumulation of damaged macromolecules during aging. Conversely, the activity of this catabolic pathway is required for lifespan extension in animal models such as *Caenorhabditis elegans* and *Drosophila melanogaster*. In this work, we describe the unexpected finding that *Zmpste24*-null mice, which show accelerated aging and are a reliable model of human Hutchinson-Gilford progeria, exhibit an extensive basal activation of autophagy instead of the characteristic decline in this process occurring during normal aging. We also show that this autophagic increase is associated with a series of changes in lipid and glucose metabolic pathways, which resemble those occurring in diverse situations reported to prolong lifespan. These *Zmpste24*^{-/-} mice metabolic alterations are also linked to substantial changes in circulating blood parameters, such as leptin, glucose, insulin or adiponectin which in turn lead to peripheral LKB1-AMPK activation and mTOR inhibition. On the basis of these results, we propose that nuclear abnormalities causing premature aging in *Zmpste24*^{-/-} mice trigger a metabolic response involving the activation of autophagy. However, the chronic activation of this catabolic pathway may turn an originally intended pro-survival strategy into a pro-aging mechanism and could contribute to the systemic degeneration and weakening observed in these progeroid mice.

INTRODUCTION

Aging is a natural process which affects most biological functions and appears to be a consequence of the accumulative action of different types of stressors. Thus, oxidative damage, telomere attrition and the decline of DNA repair and protein turnover systems are thought to be major causes of aging (1). Among the diverse events associated with this age-dependent functional decline, the accumulation of damaged proteins and organelles has been proposed to contribute in a decisive manner to cellular malfunction (2). In eukaryotic cells, there are two major pathways involved in the quality control and turnover of cellular components: the ubiquitin/proteasome system and the autophagic/lysosomal system.

The ubiquitin/proteasome system plays a major role in the maintenance of cellular homeostasis and in protein quality control, and also regulates essential processes such as cell-cycle progression or signal transduction (3,4). Nevertheless, the constitutive degradation of proteins by this ubiquitin/proteasome system is mostly limited to short-lived proteins. In contrast, the autophagic/lysosomal system is capable to degrade long-lived proteins and even entire organelles. The autophagic degradation routes can be classified into at least three different pathways: macroautophagy, microautophagy and chaperone-mediated autophagy (5,6). Macroautophagy is the major lysosomal pathway for the turnover of cytoplasmic components and will hereafter be referred to as autophagy. This process begins with the engulfment of cytoplasmic

*To whom correspondence should be addressed. Tel: +34 985104201; Fax: +34 985103564; Email: clo@uniovi.es

constituents by a membrane sac, called the isolation membrane. Then, this structure forms a double-membrane vesicle called the autophagosome which contains bulk portions of cytoplasm, and eventually fuses with the lysosome. Finally, the inner membrane of the autophagosome and its protein and organelle contents are degraded by lysosomal hydrolases and recycled.

Recently, several authors have proposed that accumulation of cellular garbage associated with aging is mainly caused by an age-related decline of autophagic and lysosomal activity (7,8). Furthermore, it has been reported that the age-related decline of autophagy is caused by the alterations in glucose metabolism and hormone levels which are inherent to aging and whose onset is delayed by calorie restriction (9,10). These observations, together with recent findings showing that autophagy genes are essential for lifespan extension in *Caenorhabditis elegans* and *Drosophila melanogaster* (11,12) and that inhibition of the *C. elegans* orthologue of TOR kinase (whose activity inhibits autophagy) doubles the lifespan of this nematode (13), support the idea that dysfunction of the autophagic catabolic pathway may contribute to aging.

Over the last few years, our knowledge of the molecular basis of aging has gained new mechanistic insights from studies on segmental progeroid syndromes in which certain phenotypes of human aging are manifested precociously or in exacerbated form. These syndromes can be classified into two major groups attending to their underlying molecular defects (14). The first group comprises premature aging disorders caused by defects in genome-stability maintenance mechanisms, such as DNA repair. Typical examples of this first group include Werner syndrome, Cockayne syndrome or trichothiodystrophy (15,16). The second group of progeroid diseases includes those caused by alterations in the nuclear envelope architecture (17–20). Thus, mutations in the *lamin A* gene or in the gene encoding the *Zmpste24*/FACE1 metalloproteinase implicated in lamin A maturation cause nuclear abnormalities that eventually lead to accelerated-aging human syndromes, such as Hutchinson-Gilford progeria, mandibuloacral dysplasia or restrictive dermopathy (17). Likewise, *lamin A* or *Zmpste24* gene disruption in mice causes premature aging syndromes (21,22). Recently, several studies have demonstrated that the nuclear envelope abnormalities that lead to accelerated aging may also contribute to normal aging (23,24), supporting the idea that the laboratory-engineered progeroid models are useful tools for studying the mechanisms underlying normal aging (25). These observations, together with the widely reported age-associated decline of autophagic potential, led us to evaluate the autophagy status in progeroid mice. In this work, we report that, surprisingly, mice with accelerated aging exhibit an extensive basal activation of autophagic degradation instead of the characteristic decline in this process occurring during normal aging. We also analyze the molecular mechanisms underlying this unexpected finding and show that the observed increase in autophagy is linked to mTOR inhibition, AMPK activation and severe metabolic alterations in glucose and lipid metabolism. These findings suggest a novel and paradoxical role of autophagic cellular degradative pathways during pathological aging processes.

RESULTS

Increased basal autophagy in progeroid mice

Previous studies have reported that basal autophagy levels are reduced in aged organisms (9,26). Likewise, the ability to induce autophagy when nutrients are scarce markedly decreases with age (27,28). To try to extend these observations to accelerated aging syndromes, we evaluated the autophagic status in different murine models of progeria. For this purpose, we first used a mouse model in which the absence of *Zmpste24* metalloproteinase leads to a progeroid phenotype which resembles many features of human premature aging syndromes (18,19). We examined the basal autophagy levels of diverse tissues from wild-type and *Zmpste24*^{-/-} mice by performing immunoblotting analysis of LC3, whose lipidation status accurately reflects autophagic activity (29). We first focused our study on skeletal muscle (quadriceps), because it has been reported that this is the most sensitive tissue to *in vivo* autophagic degradation (30). Surprisingly, the LC3 lipidation status was much higher in *Zmpste24*^{-/-} mice than in their wild-type littermates (Fig. 1A), suggesting an increase in basal autophagy levels in these progeroid mice. Nevertheless, recent studies have shown that high levels of LC3 lipidated form (LC3-II) are associated not only with an increase in the autophagic activity, but also with an impairment in autophagosome maturation (31). In this latter scenario, high LC3-II levels are accompanied by a marked increase in the level of total p62/sequestosome-1 protein. In contrast, the occurrence of a real autophagic flux increase is characterized by increased LC3-II levels together with a slight reduction of p62 protein levels (32). To test if the observed increase in LC3-II levels observed in *Zmpste24*^{-/-} mice corresponds to a real induction of the basal autophagic activity, we performed immunoblotting analyses of p62 in skeletal muscle samples from mutant and wild-type mice of the same age. As shown in Figure 1B, we could detect a slight reduction in the total p62 protein content in samples from *Zmpste24*^{-/-} mice, which confirms that the observed LC3-II accumulation in mutant mice tissues represents a *bona fide* up-regulation of the autophagic activity instead of a blockade in autophagosome maturation.

To rule out the possibility that the observed increase in autophagic activity could be an exclusive feature of skeletal muscle, we next analyzed the basal autophagic activity in other tissues from *Zmpste24*-null mice. While skeletal muscle basal autophagy was increased in the vast majority of *Zmpste24*^{-/-} mice, those with a more pronounced progeroid phenotype—as assessed by observation of weight loss, extensive alopecia and kyphosis—also showed autophagy activation in other tissues including liver and heart (Fig. 1C). These results indicate that the increase in basal autophagy observed in *Zmpste24*^{-/-} mice is not limited to skeletal muscle and follows a tissue-specific onset, which is associated with the development of the premature-aging phenotype. We next tested if the observed increase of basal autophagy in *Zmpste24*-null mice is directly provoked by prelamin A accumulation—the initial cause of accelerated aging in these mice—and not by other putative *Zmpste24* functions. For this purpose, we analyzed the basal autophagic activity of skeletal muscle from *Zmpste24*^{-/-}*Lmna*^{+/-} mice, which

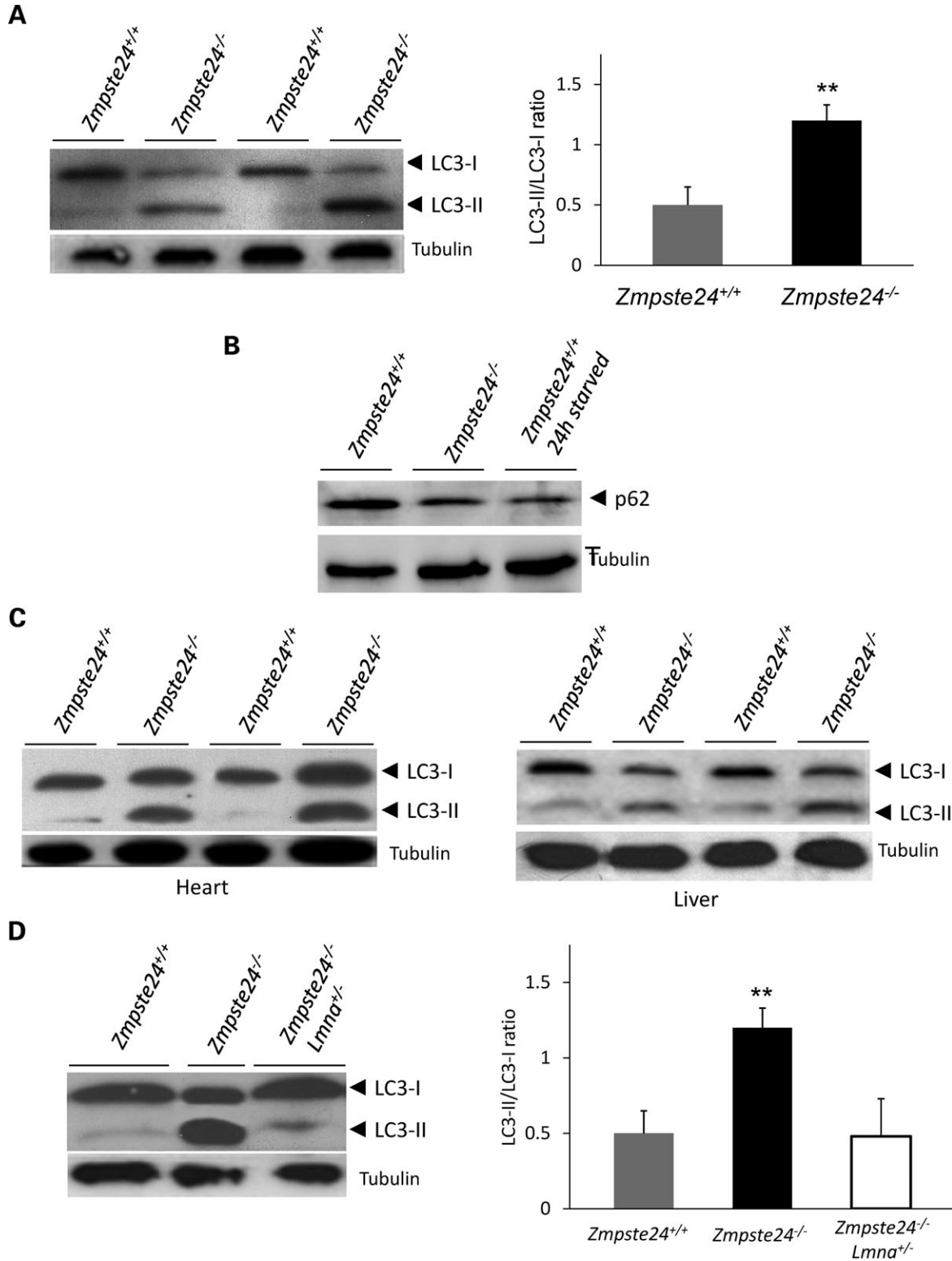


Figure 1. Disruption of Zmpste24 metalloproteinase leads to increased autophagy *in vivo*. (A) Immunoblotting analysis of LC3 lipidation status in skeletal muscle of Zmpste24-deficient mice revealed a significant increase in autophagic activity in mutant mice. (B) Representative immunoblotting analysis of p62 in skeletal muscle extracts derived from wild-type and Zmpste24-deficient mice fed *ad libitum*. Skeletal muscle samples from 24 h starved wild-type mice were used as a positive control of autophagy induction. (C) The lipidation status of LC3 is also altered in heart and liver of Zmpste24^{-/-} mice, which indicate that autophagy up-regulation in these mice is not limited to skeletal muscle. (D) The observed increase in autophagic activity is reverted in Zmpste24^{-/-} Lmna^{+/-} mice indicating that the autophagy alterations observed in progeroid mice are linked to prelamin accumulation. Error bars indicate the SEM between replicates. At least six wild-type and six mutant animals were used for each assay. * represents statistical significance ($P < 0.05$), whereas (**) represents statistical significance ($P < 0.01$), in two-tailed *t*-test.

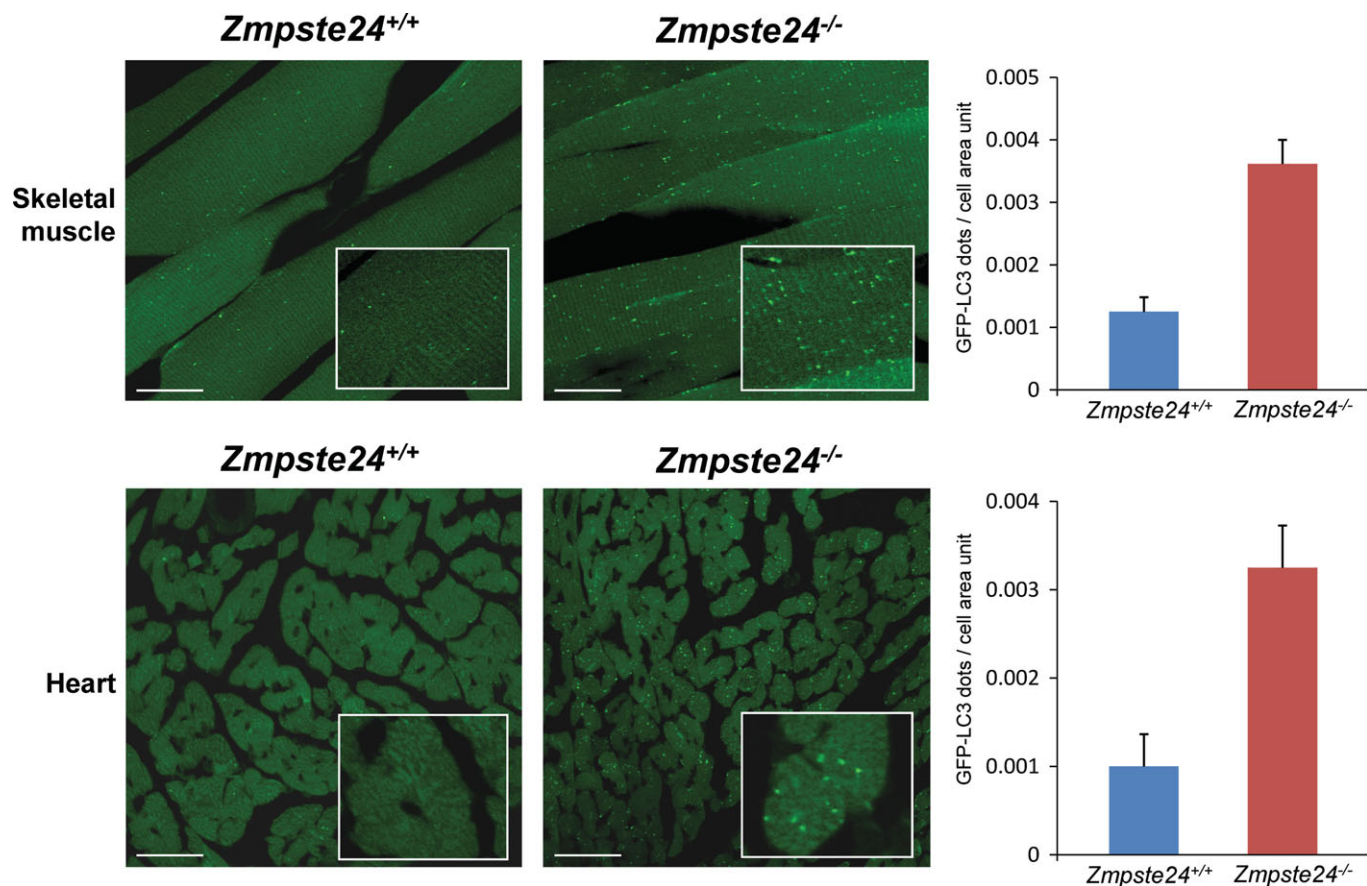


Figure 2. Fluorescent analysis of tissues from wild-type and *Zmpste24*^{-/-} GFP-LC3-expressing mice fed *ad libitum*. Representative images and quantification of skeletal muscle and heart cryosections from 3-month-old wild-type and *Zmpste24*^{-/-} mice stably expressing the GFP-LC3 transgene. Scale bars represent 50 μ m. Insets show a higher magnification of a particular area in each picture. The number of GFP-LC3 dots was counted and divided by the corresponding cellular area (right). Results shown represent the mean for five images from every tissue per mice obtained from three mice per genotype.

do not accumulate prelamin A in the nuclear envelope and exhibit a total recovery of the progeroid phenotypes characteristic of *Zmpste24*-null mice (20,22). As can be seen in Fig. 1D, muscular tissue from *Zmpste24*^{-/-}*Lmna*^{+/-} mice showed an LC3 lipidation status similar to their wild-type littermates, thus suggesting that the increase in basal autophagy observed in *Zmpste24*^{-/-} mice could be linked to the nuclear envelope abnormalities generated by the accumulation of prelamin A in the absence of its processing protease.

To confirm and extend these observations pointing to an increase of basal autophagy levels in *Zmpste24*^{-/-} progeroid mice, we crossed these mutant mice with those expressing the GFP-LC3 transgene that provides an efficient *in vivo* marker for autophagy (30). The fluorescence microscopic analysis of tissues from wild-type and mutant mice fed *ad libitum* and expressing the GFP-LC3 transgene revealed that the number of punctate GFP-LC3 structures detected in *Zmpste24*^{-/-} skeletal muscle was higher than in their corresponding wild-type littermates (Fig. 2). Moreover, and in agreement with our immunoblotting results, we could also observe an increase in the accumulation of GFP-LC3 punctate structures in other tissues, being especially evident in heart from those mutant mice with the most advanced progeroid phenotype (Fig. 2). These observations indicate that the increase in basal autophagy

observed in *Zmpste24*^{-/-} mice fed *ad libitum* presents a tissue-dependent incidence similar to the dynamics of starvation-induced autophagy, as it has been recently reported that a significant autophagy induction in heart is only observed after very long starvation periods, whereas mild starvation can induce skeletal muscle autophagy (30). Finally, it is remarkable that caloric intake was normal in *Zmpste24*^{-/-} mice as assessed by the amount of food present in their digestive track, thereby excluding malnutrition as a cause for the observed autophagic induction in these progeroid mice. This observation is also fully consistent with the fact that caloric intake is normal in Hutchinson-Gilford progeria patients despite they exhibit some anthropometric indices of malnutrition (33).

In order to extend these findings on *Zmpste24*^{-/-} progeroid mice to different murine models of accelerated aging, we evaluated the basal autophagic status in mutant mice deficient in *XPF* (34) and *CSB/XPA* (35). These mice exhibit marked features of accelerated aging caused by different deficiencies in DNA repair systems. In agreement with our previous results on *Zmpste24*^{-/-}, the basal autophagic activity in tissues from these progeroid mice was significantly higher than that observed in the same tissues from wild-type animals, as assessed by the increased LC3-II/LC3-I ratio present in progeroid mice tissues (Fig. 3). These results suggest that the increase in basal

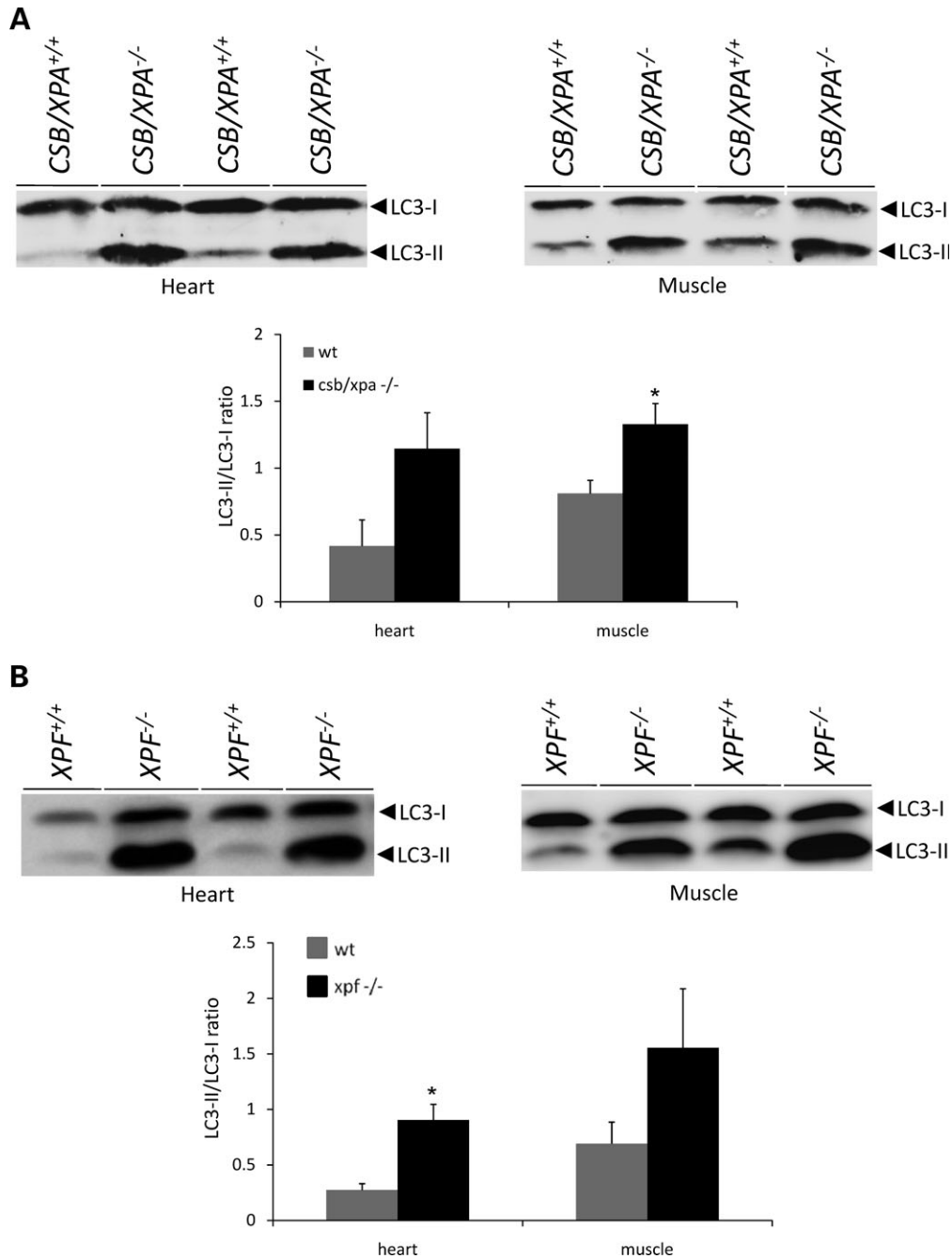


Figure 3. Activation of basal autophagy in different progeroid mice. Immunoblotting analysis of LC3 lipidation status in skeletal muscle and heart of *CSB/XPA*^{-/-} (A) and *XPF*^{-/-} mice (B) revealed a significant increase in autophagic activity in mutant mice when compared with the corresponding controls. (*) represents statistical significance ($P < 0.05$) in two-tailed *t*-test.

autophagy is not a specific alteration caused by *Zmpste24* deficiency, but a common feature of diverse premature-aging models caused by distinct molecular alterations.

Increased autophagy is linked to mTOR inhibition in *Zmpste24*^{-/-} mice

Regulation of autophagy *in vivo* is a complex process that depends on a high variety of factors. However, it is now

widely accepted that autophagy regulation mainly relies on mTOR activity, with inhibition of mTOR being a common event associated with autophagy induction (36,37). To clarify the molecular mechanisms underlying the observed autophagy increase in progeroid mouse models, we first analyzed the status of mTOR signaling pathway in *Zmpste24*^{-/-} mice. We focused our study on skeletal muscle—the tissue in which the increase in basal autophagy in *Zmpste24*^{-/-} mice is more evident—and the mTOR

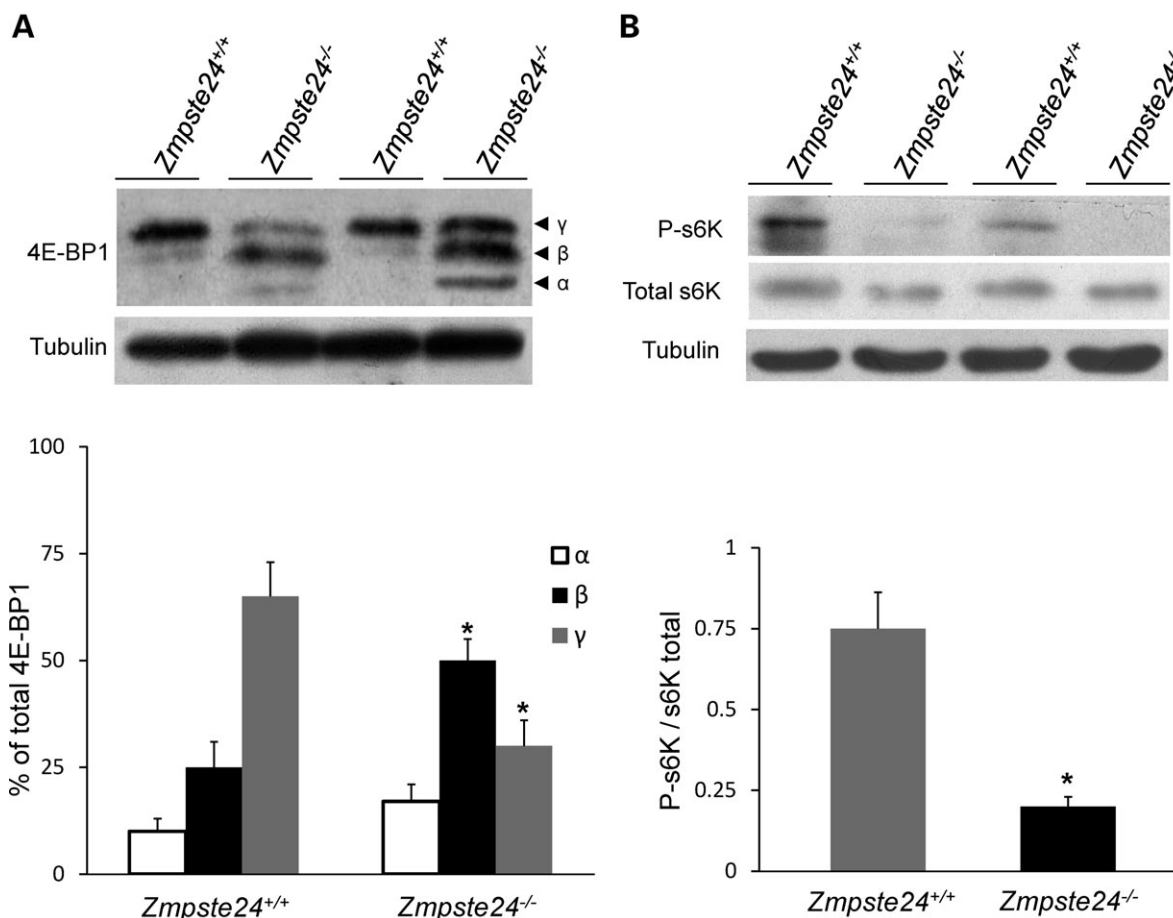


Figure 4. Autophagy up-regulation in *Zmpste24*^{-/-} mice is linked to mTOR activity down-regulation. (A) Immunoblotting analysis against the mTOR substrate, 4EBP-1, in skeletal muscle protein extracts reveals a clear decrease in the phosphorylation status of this protein, as assessed by a significant increase in its electrophoretic mobility in mutant mice. γ stands for the hyper-phosphorylated form of 4EBP-1, whereas β and α stand for medium- and low-phosphorylated forms of 4EBP-1. Densitometric analysis of these immunoblotting experiments revealed a significant decrease in the percentage of highly phosphorylated (γ) form of 4EBP-1 in mutant mice, which instead present a significantly higher percentage of β form of 4EBP-1 when compared with wild-type animals. (B) The same analysis was performed with the other major mTOR substrate, p70s6k, and also revealed a significant decrease in the phosphorylation status of this protein, which confirms that mTOR activity is down-regulated in skeletal muscle of *Zmpste24*^{-/-} mice. Error bars indicate the SEM between replicates. At least six wild-type and six mutant animals were used for each assay. (*) represents statistical significance ($P < 0.05$) in two-tailed *t*-test.

activity was monitored by analyzing the phosphorylation levels of its two main downstream targets: 4E-BP1 and p70-S6K (38,39). The immunoblotting analysis of 4E-BP1 in skeletal muscle protein extracts revealed a clear decrease of 4E-BP1 phosphorylation in *Zmpste24*^{-/-} mice when compared with wild-type animals (Fig. 4A), indicating a down-regulation in the activity of mTOR. To further confirm this observation, we analyzed the phosphorylation status of p70-S6K, the other major mTOR substrate. Phosphorylation of p70-S6K at Thr389 has been widely described to reflect mTOR activity (40). Consistent with the above results on 4E-BP1 phosphorylation, we detected a clear decrease in the phosphorylation of p70-S6K at Thr389 in *Zmpste24*^{-/-} muscle (Fig. 4B), thus confirming that mTOR activity is down-regulated in *Zmpste24*^{-/-} mice. Taken together, these results demonstrate that the up-regulation of basal autophagy observed in *Zmpste24*^{-/-} mice is linked to mTOR pathway inhibition.

mTOR inhibition and increased basal autophagy in *Zmpste24*^{-/-} mice are linked to LKB1-AMPK activation

To elucidate the molecular mechanisms underlying the mTOR inhibition and the subsequent autophagy activation observed in *Zmpste24*^{-/-} mice, we analyzed the status of the signaling pathways involved in mTOR regulation. There are two major routes controlling mTOR activity *in vivo*: the PI3K-Akt pathway which mediates the activation of mTOR in response to growth factors, and the LKB1-AMPK pathway which is involved in mTOR activity inhibition in response to nutritional, genotoxic and metabolic stress signals (41,42). To monitor the PI3K-Akt pathway, we evaluated the status of two of its main regulators *in vivo*, Akt and PTEN. Phosphorylation of Akt at Thr308 is considered as an indicator of Akt activity (43), whereas the cellular levels of PTEN, a major negative regulator of this signaling pathway, are inversely associated with Akt activity (44).

As shown in Figure 5A, we found no appreciable changes in the phosphorylation of Akt at Thr308 in skeletal muscle from *Zmpste24*^{-/-} and wild-type mice. Similar results were obtained for PTEN, as assessed by the finding that total protein levels of this phosphatase were comparable in mice from both genotypes (Fig. 5B). These results strongly suggest that the mTOR pathway inhibition observed in *Zmpste24*-null mice is not a consequence of a decrease in the activity of the PI3K-Akt signaling pathway.

Then, we analyzed the activity of the LKB1-AMPK signaling pathway to test whether a possible alteration in this route could account for the mTOR inhibition observed in *Zmpste24*^{-/-} mice. For that purpose, we first examined the phosphorylation status of AMPK α at Thr172, which has been widely used to monitor AMPK activity *in vivo* (45). As can be seen in Figure 5C, we found that AMPK phosphorylation was significantly higher in *Zmpste24*^{-/-} than in controls, which indicates an increase of AMPK activity in these mutant mice. To further clarify the molecular basis underlying this observation, we analyzed the total protein content of LKB1—the main kinase involved in AMPK phosphorylation—as the cellular levels of this kinase are correlated with AMPK activity (46). As shown in Figure 5D, *Zmpste24*^{-/-} mice show a significantly higher LKB1 protein levels than wild-type animals, as measured by immunoblotting analysis, thereby confirming that the activity of the LKB1-AMPK signaling pathway is up-regulated in these mice. Taking together these results, we conclude that the observed basal autophagy increase and mTOR inhibition in *Zmpste24*^{-/-} progeroid mice are linked to an up-regulation of the LKB1-AMPK pathway and not to a decrease in PI3K-Akt signaling.

Increased basal autophagy and mTOR inhibition in *Zmpste24*^{-/-} mice are not dependent on p53 activation

Recent studies have shown that genotoxic stress and DNA damage can promote autophagy through a p53-dependent mechanism which involves AMPK-dependent mTOR inhibition (47,48). It has also been recently reported that accelerated aging in *Zmpste24*^{-/-} mice is linked to p53 signaling activation (20). In addition, we have observed that the activity of autophagic activity modulators, such as mTOR and AMPK, is not altered in p53-deficient mice when compared with wild-type animals (data not shown). These facts prompted us to test the possibility that the increase in p53 signaling activity in *Zmpste24*^{-/-} mice could account for the observed LKB1-AMPK pathway activation and its subsequent effects on mTOR and autophagy. For this purpose, we generated *Zmpste24*^{-/-}*p53*^{-/-} mice, which show a partial recovery of the progeroid phenotype associated with *Zmpste24*^{-/-} deficiency. Thus, using skeletal muscle protein extracts derived from these double mutant mice, we performed immunoblotting analysis to check the status of LKB1 and AMPK in the absence of p53. As can be seen in Figure 6A, total LKB1 protein levels in double mutant extracts were similar to those detected in *Zmpste24*^{-/-} expressing p53 (Fig. 6A). Consistently, the lack of p53 did not revert the increase in the phosphorylation status of AMPK caused by *Zmpste24* deficiency (Fig. 6B) and similar results were obtained when we analyzed

LC3 lipidation levels and 4E-BP1 phosphorylation status in extracts derived from double mutant mice (Fig. 6B–C). Taken together, these results suggest that the observed alterations linked to the excessive basal autophagy of *Zmpste24*^{-/-} mice are independent of p53 activity.

LKB1-AMPK signaling activation in *Zmpste24*^{-/-} mice is linked to changes in circulating levels of glucose and blood hormones

The above findings, which indicate that p53 is not involved in the activation of AMPK signaling in *Zmpste24*^{-/-} mice, prompted us to analyze circulating plasma levels of hormones and other biochemical parameters which have also been reported to modulate the activity of this kinase (49,50). As shown in Figure 7, different plasma parameters were clearly altered in *Zmpste24*^{-/-} mice when compared to control mice. Thus, blood glucose concentration and plasma levels of insulin and leptin were significantly reduced in these mutant mice, whereas adiponectin levels were higher in *Zmpste24*^{-/-} mice than in their wild-type littermates. Because previous studies have established that a decrease in blood glucose levels and an increase of circulating adiponectin act as *in vivo* inducers of AMPK activity (51), the elevated LKB1-AMPK activity observed in *Zmpste24*^{-/-} mice may be caused by the low glucose levels and high plasma adiponectin concentration found in these mutant mice.

Alterations of glucose and lipid metabolic pathways in *Zmpste24*^{-/-} mice

The finding that *Zmpste24*^{-/-} mice present marked alterations in different blood parameters related to glucose and lipid homeostasis suggests that metabolic pathways involved in these processes could be also altered in these animals. To examine this possibility, we first performed full transcriptome analysis of *Zmpste24*^{-/-} mice liver, as this tissue is a major modulator of glucose and lipid homeostasis *in vivo*. As shown in Supplementary Material, Figs S1 and S2, several genes involved in relevant processes for glucose and lipid metabolism such as TCA cycle, glycolysis, gluconeogenesis, fatty acid synthesis and fat accumulation present altered expression levels in *Zmpste24*^{-/-} mice liver when compared with wild-type mice. To further confirm the observed alterations, we performed qPCR analysis of a series of key genes involved in the regulation of these processes (Fig. 8A–C). We first analyzed the mRNA transcript levels of relevant genes for gluconeogenesis, such as *Pepck* and *G6Pase*, encoding phosphoenolpyruvate carboxykinase and glucose-6-phosphatase, respectively. As can be seen in Figure 8A, both genes were up-regulated in liver from *Zmpste24*^{-/-} mice, indicating that this process is enhanced in mutant animals. In contrast, the fact that the expression of *Pk* (pyruvate kinase), a key gene for glycolysis regulation, is not altered in mutant mice suggests that glycolysis rate is not up-regulated in these animals. Next, we analyzed mRNA levels of important genes for glycogen metabolism such as *Gck* and *Gys2* that encode glucokinase and hepatic glycogen synthase, respectively. Although *Gys2* mRNA levels were not altered in mutant mice livers, *Gck* expression was clearly up-regulated in *Zmpste24*-deficient mice (Fig. 8A).

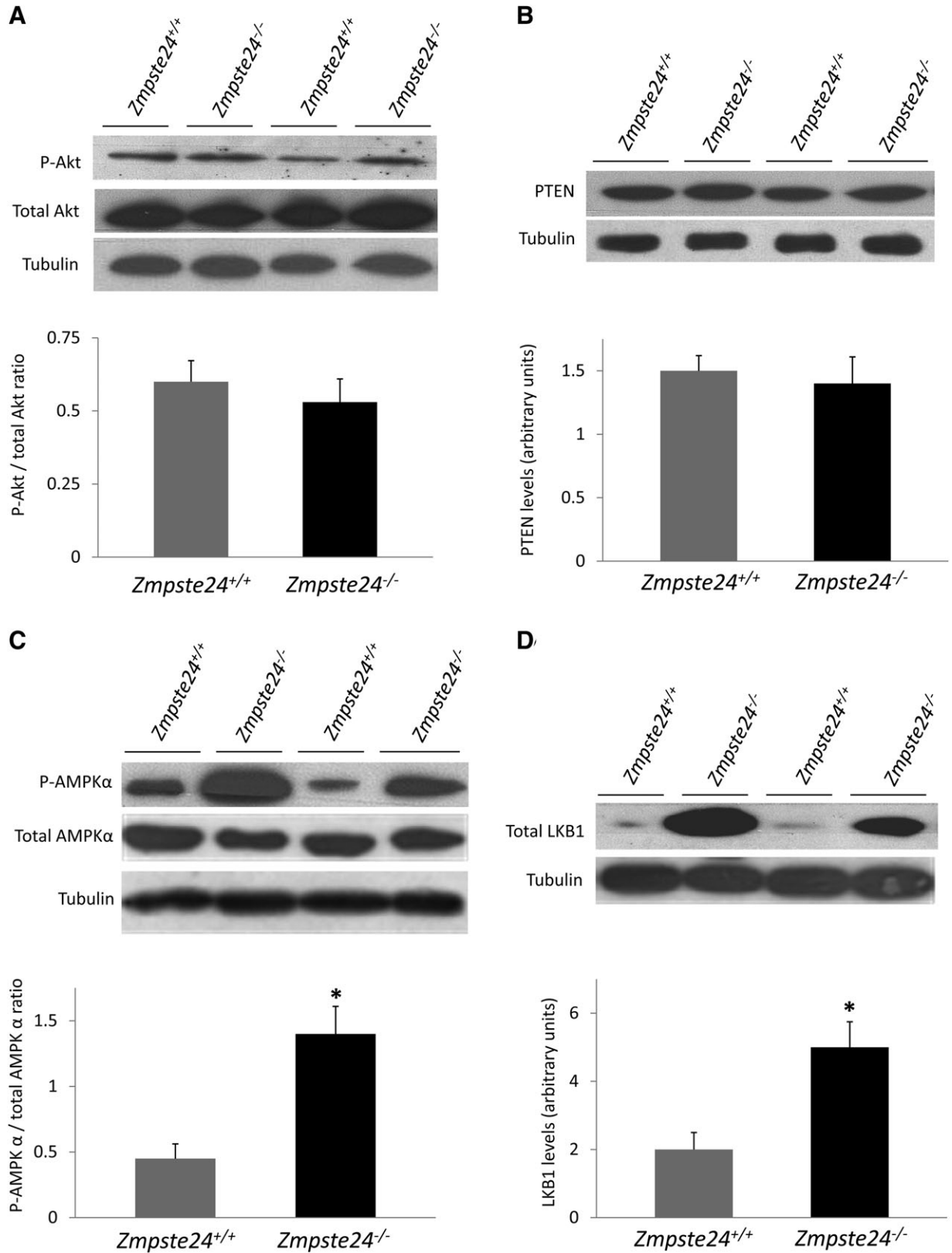


Figure 5. Autophagy increase in *Zmpste24*^{-/-} mice is related to changes in LKB1-AMPK activity but not in PI3K-Akt signalling. Immunoblotting analysis of skeletal muscle protein extracts from wild-type and mutant mice revealed that neither Akt phosphorylation status (A) nor PTEN total protein levels (B) are significantly altered in *Zmpste24*^{-/-} mice. However, AMPKα phosphorylation status (C) and LKB1 protein content (D) are significantly higher in mutant mice, suggesting a connection between autophagy up-regulation and LKB1-AMPK signaling enhancement in these animals. Error bars indicate the SEM between replicates. At least six wild-type and six mutant animals were used for each assay. (*) represents statistical significance ($P < 0.05$) in two-tailed *t*-test.

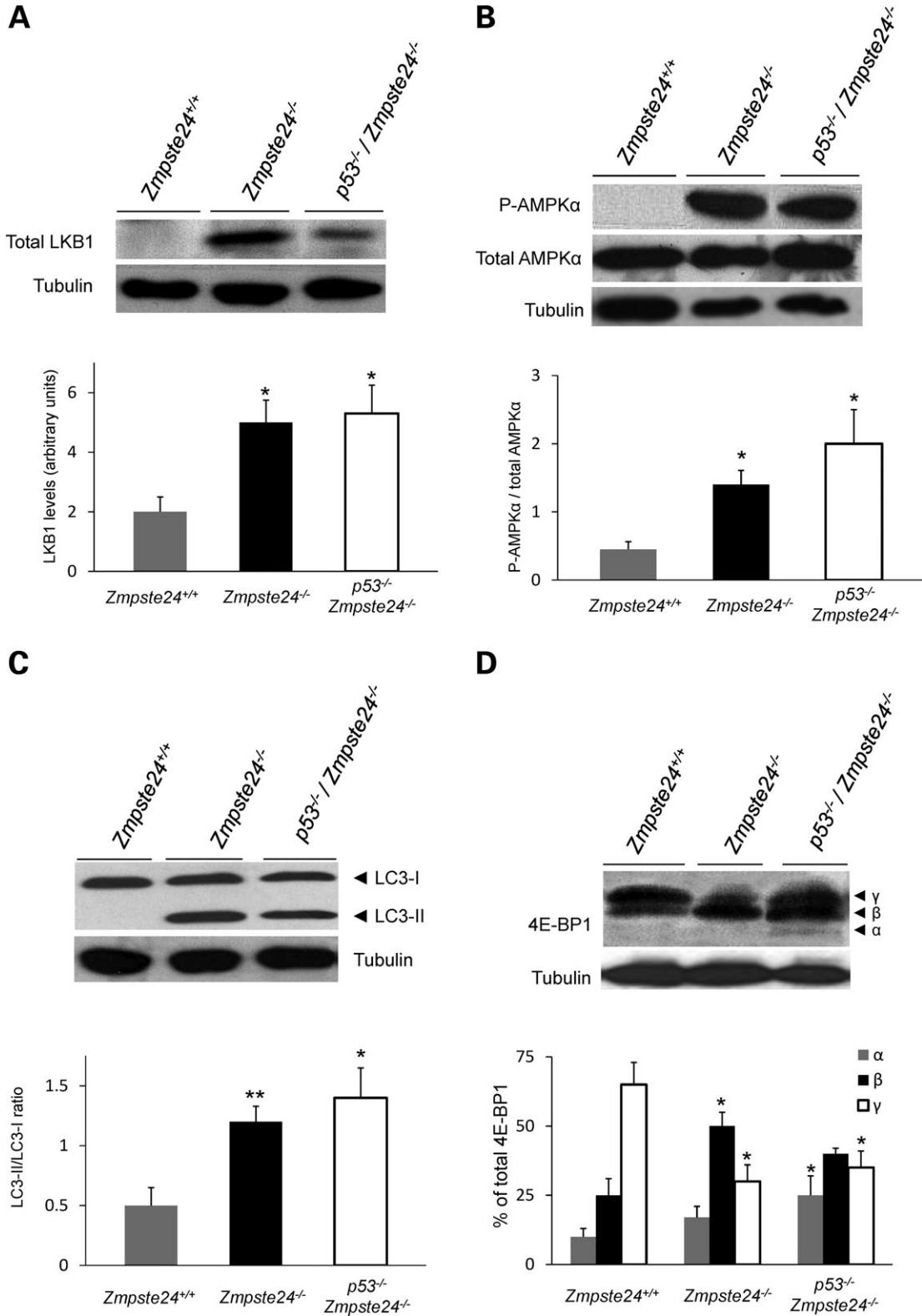


Figure 6. p53 pathway is not involved in the autophagy-related alterations of *Zmpste24*^{-/-} mice. LKB1 protein levels (A), AMPK phosphorylation (B), 4EBP1 phosphorylation (γ stands for the hyper-phosphorylated form of 4EBP-1, whereas β and α stand for medium- and low-phosphorylated forms of 4EBP-1) (C) and LC3 lipidation status (D) of *Zmpste24*^{-/-} mice do not significantly change in a *p53*-null background. Error bars indicate the SEM between replicates. At least four wild-type and four mutant animals were used for each analysis. (*) represents statistical significance ($P < 0.05$), whereas (**) represents statistical significance ($P < 0.01$) in two-tailed *t*-test when compared with wild-type mice values.

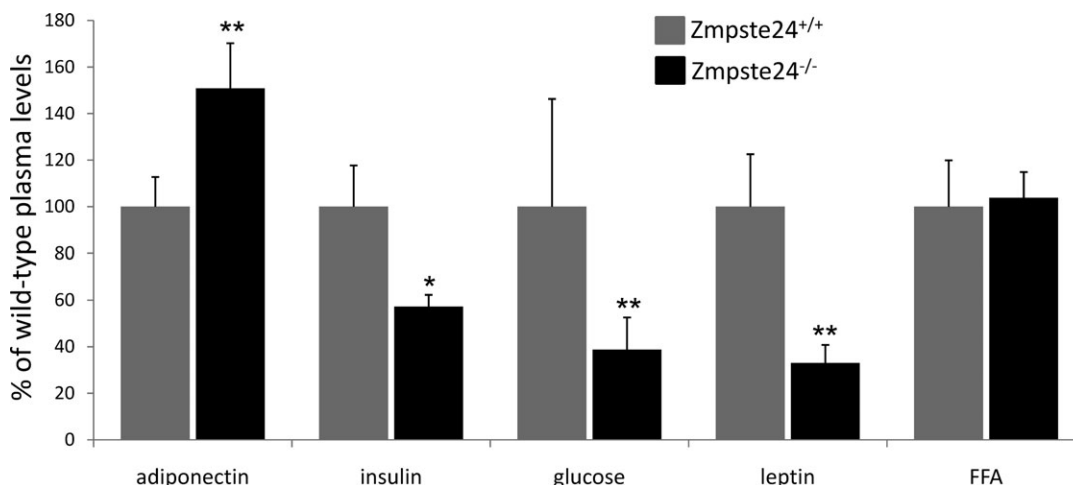


Figure 7. Plasma hormone levels and blood glucose concentration are altered in *Zmpste24*^{-/-} mice. Plasma adiponectin levels are significantly increased in 10-week-old *Zmpste24*^{-/-} mice, when compared with their corresponding controls. In contrast, plasma levels of insulin and leptin are significantly reduced in these mice. Similarly, blood glucose concentration is lower in mutant animals, whereas free fatty acid plasma levels do not differ substantially between wild-type and progeroid mice. Error bars indicate the SEM between replicates. At least six wild-type and six mutant animals were used for each assay. (*) represents statistical significance ($P < 0.05$), whereas (**) represents statistical significance ($P < 0.01$) in two-tailed *t*-test.

This observation suggests that the flux of glucose derived from an up-regulation in the gluconeogenic pathway does not contribute to restore glycaemia in *Zmpste24*^{-/-} mice. Instead, it likely re-enters to mouse tissues and is converted again into glucose-6-phosphate, an allosteric activator of glycogen synthase when produced by glucokinase and whose increase is associated with a higher rate of glycogen synthesis (52). In fact, *Zmpste24*-null mice show a clear increase in liver glycogen content, when compared with wild-type littermates (Fig. 8D), which is consistent with previous works reporting an increase in glycogen synthesis after glucokinase overexpression (53).

Regarding genes important for lipid metabolism, we observed an up-regulation of *Fas* and *Acc1* which encode fatty acid synthase and acyl-coenzyme A carboxylase, respectively (Fig. 8B), suggesting that fatty acid synthesis is increased in livers from *Zmpste24*^{-/-} mice. This increase in fatty acid synthesis could provide an alternative energy source through an increase in fatty acid mitochondrial β -oxidation. In fact, mRNA levels of key genes for this process as *Mcad* or *Cpt1a*, encoding medium chain acyl CoA dehydrogenase and carnitine palmitoyltransferase 1A, respectively, are also up-regulated in mutant mice. All these alterations in lipid synthesis and metabolism finally lead to an extensive accumulation of fatty acids in the liver, as revealed by Oil Red staining, which reveals the occurrence of a clear steatosis in mutant mice livers when compared with their wild-type littermates (Fig. 7E).

After these findings indicating the occurrence of marked alterations of glucose and lipid metabolism in *Zmpste24*^{-/-} mice, we analyzed the status of the transcriptional co-activator Pgc-1 α (peroxisome proliferator-activated receptor- γ co-activator-1 α), an essential regulator of hepatic gluconeogenesis (54) and fatty acid oxidation (55). As shown in Figure 8C, *Pgc1 α* mRNA levels were significantly higher in liver from *Zmpste24*-deficient mice than in the corresponding wild-type controls, which could account for the observed increase in the expression of gluconeogenic and beta oxidation-related genes in *Zmpste24*^{-/-} mice (Fig. 8C).

Likewise, *Pdk4* (pyruvate dehydrogenase kinase-4), one of the main Pgc-1 α targets (55,56) and a key regulatory enzyme involved in switching the energy source from glucose to fatty acids (57) was strikingly up-regulated in mutant mice (Fig. 7C). These observations suggest that the metabolic activities regulated by Pgc-1 α are enhanced in these progeroid mice, shifting their glucose and lipid metabolism to a situation similar to starvation.

In summary, the alteration in the expression levels of metabolic regulators, as Pgc-1 α , together with additional putative alterations in other transcription factors, might underlie the reported metabolic changes of *Zmpste24*^{-/-} mice and explain the dysregulation in the expression levels of key genes for distinct metabolic pathways involved in glucose and lipid homeostasis. This complex metabolic dysfunction leads to substantial changes in circulating hormones and biochemical parameters. These changes probably account for the initially observed increase in basal autophagy, mTOR inhibition and AMPK-LKB1 axis up-regulation and could contribute to explain the growth defects and progressive loss of weight characteristic of premature-aging syndromes.

DISCUSSION

Multiple studies have shown that proteolytic activities decrease with age, a situation which leads to the accumulation of damaged macromolecules during physiological aging (9,10). Contrary to this well-established concept, in this work we provide evidence that mice with premature aging caused by nuclear lamina alterations exhibit a marked activation of autophagic proteolysis. Likewise, mice with accelerated aging caused by defects in DNA repair systems also show an induction of autophagy. Additionally, we describe that the increase in autophagy observed in *Zmpste24*^{-/-} progeroid mice is linked to AMPK activation and mTOR inhibition, transcriptional changes in key genes for lipid and glucose

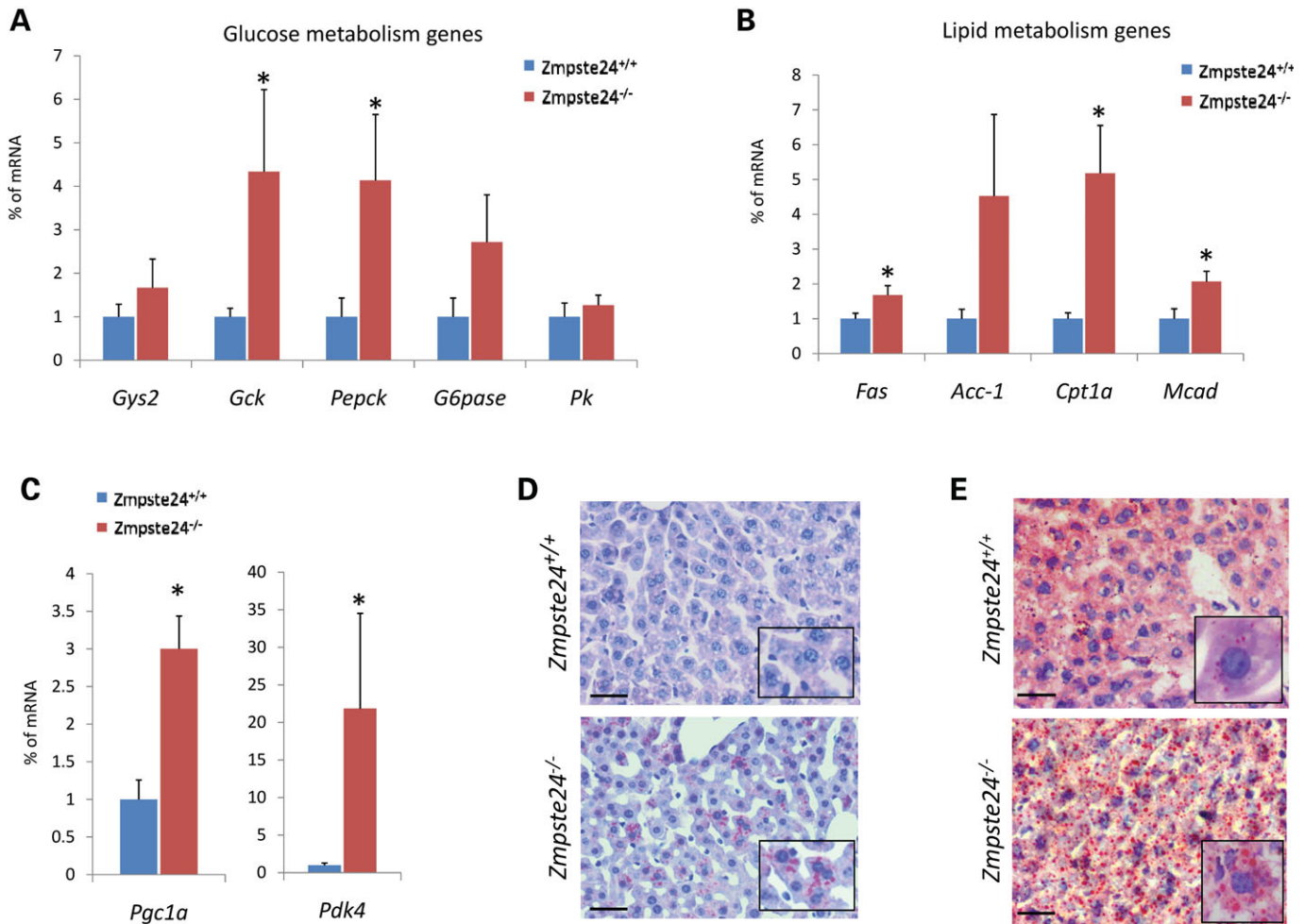


Figure 8. Glucose and lipid metabolism analysis in liver from *Zmpste24*^{-/-} mice. (A) qPCR evaluation of mRNA levels of key genes for gluconeogenesis (*Glc-6-Pase*, *Pepck*), glycolysis (*pyruvate kinase*) and glycogen metabolism (*glycogen synthase 2*, *glucokinase*) in liver. (B) qPCR analysis of mRNA levels of key genes for fatty synthesis and β -oxidation in liver. (C) qPCR evaluation of mRNA levels for *Pgc-1 α* and *Pdk4* in liver. Error bars indicate the SEM between replicates. At least eight wild-type and eight mutant animals were used for each assay. (*) represents statistical significance ($P < 0.05$) in two-tailed *t*-test. (D) Representative images of PAS staining of liver cryosections showing a clear increase in glycogen content in liver from *Zmpste24*^{-/-} mice when compared with their wild-type littermates. (E) Representative images of oil red staining of liver cryosections showing a clear increase in lipid content in liver from *Zmpste24*^{-/-} mice when compared with controls. Scale bars represent 50 μ m. Insets show a higher magnification of a particular area in each picture.

metabolism regulation, and alterations in levels of different serum factors including glucose, insulin and adiponectin. All these observations are consistent with the possibility that nuclear abnormalities causing premature aging in *Zmpste24*-null mice trigger a protective metabolic response aimed at attenuating the deleterious consequences associated with the development of progeroid syndromes.

Remarkably, the induction of this autophagic response and the concomitant metabolic changes observed in *Zmpste24*^{-/-} mice are commonly associated with longer lifespan rather than with the shortened longevity characteristic of these progeroid animals. Thus, autophagy is primarily a pro-survival mechanism which generates nutrients and protects cells from the age-induced accumulation of altered proteins, membranes and organelles (5,6). The anti-aging function of autophagy is also supported by the finding of a marked decline of this catabolic process during adulthood, and its virtually negligible presence at older age (9,10). The unexpected activation of this

pro-survival catabolic pathway in premature aging *Zmpste24*-null mice prompted us to consider its putative relationship with the metabolic changes occurring in these animals. We first found that mTOR activity was strongly inhibited in *Zmpste24*^{-/-} mice, which is consistent with the observed autophagy increase in these mutant animals, as mTOR is an inhibitor of the autophagic proteolytic pathway (58). The mTOR inhibition observed in *Zmpste24*-null mice is also in agreement with the proposed occurrence of an anti-aging mechanism in these progeroid mice, since inhibition of TOR-signaling increases lifespan in yeast and nematodes (13,59). The activation of the LKB1-AMPK pathway in *Zmpste24*^{-/-} mice is also consistent with this possibility as it has been described that LKB1 and AMPK cooperate during conditions of metabolic stress to establish cell-cycle quiescence in the stem cell compartment, thus contributing to prolong lifespan (60). Likewise, overexpression of AMPK promotes lifespan extension in *C. elegans*, reinforcing the idea that this kinase

may act as a positive regulator of longevity (61,62). The observed alterations in glucose homeostasis in *Zmpste24*-null mice—which show hypoglycemia and hypoinsulinemia—are also features associated with extended lifespan in diverse model organisms (63,64). The fact that these alterations are linked to a shift in the transcriptional profile of several key genes for regulation of metabolism also agrees with our proposal of a general anti-aging metabolic response in *Zmpste24*^{-/-} mice aimed at storing resources in an attempt to preserve their somatic integrity. In this regard, it has recently been reported that accumulation of progerin—a mutant isoform of lamin A whose expression leads to the development of Hutchinson-Gilford progeria (65,66)—causes abnormal chromosome segregation and binucleation after mitosis (67,68). Thus, it is tempting to speculate that a normal growth rate in the presence of progerin or prelamin A accumulation would compromise somatic integrity. In fact, the metabolic shift observed in *Zmpste24*^{-/-} mice, which shares many features with those observed in animals subjected to calorie-restriction, seems a reasonable strategy to slow down the cellular division-dependent accumulation of damage present in these animals. Remarkably, all the reported alterations, which finally lead to basal autophagy up-regulation are manifested during postnatal development and exacerbated with age in *Zmpste24*^{-/-} mice, which strongly suggests that they represent a systemic and progressive response rather than a constitutive deficiency in these mutant animals. In fact, all metabolic alterations reported in this work are already present at certain extent when the first progeroid features (weight loss, alopecia and kyphosis) are noticed in *Zmpste24*^{-/-} mice, and their magnitude increases in parallel to the development of the progeroid phenotype. Lastly, the fact that this response does not occur in *Zmpste24*^{-/-}*Lmna*^{+/-} mice—which do not accumulate prelamin A in the nuclear envelope and lack the progeroid phenotype characteristic of *Zmpste24*^{-/-} mice (20)—provides strong evidence about the causal involvement of nuclear architecture abnormalities in triggering this anti-aging mechanism.

Interestingly, very recent and elegant studies have shown that progeroid mice with defects in different DNA repair genes exhibit an adaptive metabolic response characterized by alterations in the glucose/insulin pathway, which are very similar in some aspects to that reported herein for *Zmpste24*-null mice (35,69,70). It has been proposed that this response is aimed at re-allocating resources from growth to somatic preservation and life extension, a situation which shows clear parallels with that proposed to occur in *Zmpste24*^{-/-} mice. In fact, there are many similarities among the metabolic alterations present in different models of premature aging caused by defects in DNA repair mechanisms and those described herein for *Zmpste24*^{-/-} mice. The observed up-regulation of gluconeogenic and beta-oxidative pathways are part of the metabolic alterations shared by these two types of premature aging murine models. Our novel observation that autophagy is also markedly induced in all these progeroid models suggests that activation of this pathway might be a common determinant in the metabolic response triggered by diverse conditions causing premature aging. Furthermore, the finding of an increased autophagy in this putative protective response might also be of interest in an evolutionary context, since this process appears to have evolved in eukaryotes as part of a stress response to deal with

environmental pressures such as those derived from nutrients scarcity (6,36). Accordingly, autophagy-deficient *Atg5*^{-/-} mice do not survive to the food shortage occurring during neonatal starvation (71). Our finding that autophagy may also be activated in adult tissues by the accumulation of damage in the nuclear architecture suggests the adaptation of this pro-survival pathway to a condition very different from its original function as a mechanism to increase the possibilities of eukaryotic organisms to survive metabolic stress (36). Thus, a proteolytic pathway that generates ATP and favors transition from prenatal to postnatal environment could also serve to adaptively retard aging and improve organismal homeostasis when triggered in adult tissues. Nevertheless, it is clear that this adaptive response is unable to repair or at least to compensate for the profound nuclear architecture defects derived from prelamin A accumulation in *Zmpste24*^{-/-} mice, and these persistent defects lead to the premature death of these mutant mice.

Finally, the somewhat paradoxical finding that autophagic proteolysis is up-regulated in *Zmpste24*^{-/-} mice and in other models of accelerated aging may also provide new insights into the mechanisms underlying the multiple tissue alterations observed in these mice as well as in the related human progeroid syndromes caused by nuclear lamina abnormalities. Thus, and in addition to the above discussed relevance of autophagy to facilitate temporary survival to metabolic stress, this catabolic pathway can also be detrimental and lead to cell death when chronically activated (72,73). This situation could contribute to the progressive loss of muscular mass that ultimately leads to the muscular dystrophy phenotype observed in both *Zmpste24*-null mice and progeria patients (18,22). Further studies with specific autophagy inhibitors or with appropriate animal models of autophagy-deficiency will be helpful to clarify whether the observed increase of basal autophagic activity in *Zmpste24*^{-/-} mice is able to counteract the progression of their progeroid phenotype, or by contrast, contributes to the development of the multiple pathologies observed in these mice.

In summary, on the basis of the results presented herein, we propose a model in which the nuclear architecture defects occurring in *Zmpste24*^{-/-} progeroid mice activate an anti-aging response first characterized by transcriptional alterations in metabolism regulatory genes and profound changes in circulating blood glucose and hormone levels. These changes likely lead to activation of the LKB1-AMPK pathway and to the subsequent inhibition of mTOR, which in turn results in activation of autophagy, an essential component of pro-survival pathways in eukaryotic organisms. However, the occurrence of persistent nuclear architecture defects in all cells from *Zmpste24*^{-/-} mutant mice turns this temporally regulated response into a chronic situation. This fact probably potentiates the detrimental consequences of this pro-survival mechanism and may finally overcome its beneficial anti-aging effects. It will be very interesting to explore the possibility that a similar metabolic checkpoint to that reported herein for *Zmpste24*^{-/-} mice could operate in patients affected by devastating human progeroid syndromes such as Hutchinson-Gilford disease, which are also caused by defects in nuclear lamina architecture (14,17,18). Finally, the recent observation that nuclear envelope abnormalities could also be a central cause of aging (23) opens the possibility that normal physiological aging or senescence-involving conditions

may engage a similar response involving the chronic activation of autophagy, an originally intended pro-survival strategy that may finally turn out into a pro-aging mechanism.

MATERIALS AND METHODS

Transgenic animals

Mutant mice deficient in *Zmpste24* metalloproteinase and transgenic mice expressing the fluorescent autophagosome marker GFP-LC3 have been previously described (22,30). *Lmna*^{-/-}, *p53*^{-/-}, *XPF*^{-/-} and *CSB/XPA*^{-/-} mice were kindly provided by Drs C. Stewart (NIH, USA), M. Serrano (CNIO, Spain), M. Blasco (CNIO, Spain) and J. Hoeijmakers (Erasmus University, Netherlands). Animal experiments were conducted in accordance with the guidelines of the Committee on Animal Experimentation of the Universidad de Oviedo, Oviedo, Spain.

Immunoblotting analysis

Mice tissues were immediately frozen in liquid nitrogen after extraction and were homogenized in a 20 mM Tris buffer pH 7.4, containing 150 mM NaCl, 1% Triton X-100, 10 mM EDTA and Complete® protease inhibitor cocktail (Roche Applied Science, Mannheim, Germany). Once homogenized, tissue extracts were centrifuged at 12000 g and 4°C, and supernatants were collected. The protein concentration of the supernatant was evaluated by bicinchoninic acid technique (BCA protein assay kit, Pierce Biotechnology, Rockford, IL, USA). Twenty-five microgram of each protein sample was loaded on 13% SDS-polyacrylamide gels. After electrophoresis, gels were electro-transferred onto nitrocellulose filters, and then the filters were blocked with 5% non-fat dried milk in PBT (phosphate buffered saline with 0.05% Tween 20) and incubated with primary antibodies in 5% BSA in PBT. After three washes with PBT, filters were incubated with horseradish peroxidase-conjugated goat anti-rabbit IgG at a 1:10000 dilution in 1.5% milk in PBT, and developed with a West Pico enhanced chemiluminescence kit (Pierce Biotechnology). The antibody against LC3 was kindly provided by Dr T. Ueno (Juntendo University, Tokyo, Japan). The antibodies against LKB1 and p62 were from Upstate (Manchester, UK), and Progen Biotechnik (Heidelberg, Germany), respectively. All the other antibodies used in this work were from Cell Signaling (Beverly, MA, USA).

Quantitative analysis of GFP-LC3 dots

Mutant mice deficient in *Zmpste24* metalloproteinase were crossed with transgenic mice overexpressing GFP-LC3 that provide an efficient *in vivo* marker for autophagy (30). To avoid autophagy induction during manipulation of mice, they were perfused with 4% paraformaldehyde in 0.1 M sodium phosphate buffer (PBS), pH 7.4. Tissues were harvested and further fixed with the same fixative solution for at least 4 h, followed by treatment with 15% sucrose in PBS for 4 h, and then with 30% sucrose solution overnight. Tissue samples were embedded in Tissue-Tek OCT compound (Sakura Finetechnical Co. Ltd, Tokyo, Japan) and stored at -70°C. Samples were

then sectioned at 5 µm thickness with cryostat (CM3050 S, Leica, Deerfield, IL, USA), air-dried for 1 h, washed in PBS for 5 min, dried at RT for 30 min and mounted with conventional anti-fading medium. The number of GFP-LC3 dots was counted in five independent visual fields from at least five independent mice in each organ using a Leica TCS sp2 AOBs confocal fluorescence microscope.

Blood and plasma parameters

Animals were starved for 5 h to avoid any possible alteration in blood glucose levels due to food intake previous to measurements. Blood glucose was measured with an Accu-Chek glucometer (Roche Diagnostics, Barcelona, Spain) using blood from the tail vein. For the other measured parameters, blood was extracted directly from the heart after anesthetizing mice with halothane. Plasma was obtained as previously described (74). Briefly, blood was immediately centrifuged after collection at 3000 g and 4°C and the supernatant was collected and stored at -70°C until analysis. For plasma leptin, adiponectin and insulin measurements, we used Linco Diagnosis ELISA Kits, whereas for free fatty acids levels determination we used Wako NEFA-C colorimetric test (WAKO Chemicals, Tokyo, Japan). All protocols were performed according to manufacturer's instructions.

RNA preparation

Collected tissue was immediately homogenized in TRI reagent (Sigma, Poole, UK) and processed in the same day through alcohol precipitation according to the manufacturer directions. RNA pellets were then washed in cold 80% ethanol and stored at -80°C until further use. Following re-suspension of RNA in nuclease-free water (Ambion, Austin, TX, USA), the samples were quantified and evaluated for purity (260 nm/280 nm ratio) using a NanoDrop ND-1000 spectrophotometer (NanoDrop Technologies, Wilmington, DE, USA) and 100 µg of each sample was further purified using RNeasy spin columns according to the manufacturer's instructions (Qiagen, Valencia, CA, USA).

Quantitative RT-PCR analysis

cDNA was synthesized using 1 to 5 µg of total RNA, 0.14 mM oligo(dT) (22-mer) primer, 0.2 mM concentrations of each deoxynucleoside triphosphate and Superscript II reverse transcriptase (Invitrogen, Carlsbad, CA, USA). Quantitative reverse transcription-PCR (qRT-PCR) was carried out in triplicate for each sample using 20 ng of cDNA, TaqMan® Universal PCR master mix (Applied Biosystems, San Francisco, CA, USA), and 1 µl of the specific TaqMan® custom gene expression assay for the gene of interest (Applied Biosystems). To quantitate gene expression, PCR was performed at 95°C for 10 min, followed by 40 cycles at 95°C for 15 s, 60°C for 30 s and 72°C for 30 s using an ABI Prism 7700 sequence detector system. As an internal control for the amount of template cDNA used, gene expression was normalized to the mouse β-actin gene using the Mouse β-actin Endogenous Control (VIC®/MGB Probe, Primer Limited) TaqMan® Gene expression assay (Applied Biosystems). Relative expression of the distinct

analyzed genes was calculated according to manufacturer's instructions. Briefly, the analyzed gene expression was normalized to β -actin in wild-type or *Zmpste24*^{-/-} derived samples, using the following formula: the mean values of $2^{\Delta\text{CTgene}}$ ($\text{Gene of interest} - \Delta\text{CTgene} (\beta\text{-actin})$) for at least six different wild-type animals were considered 100% for each analyzed gene and the same values for *Zmpste24*^{-/-} mice tissues were referred to those values as previously described (75).

Transcriptome analysis

The full transcriptome analysis was conducted using Affymetrix mouse 430_2 expression gene-arrays according to the protocols recommended by the manufacturer (Affymetrix, Santa Clara, CA, USA). Three male mice from each phenotype maintained under the same feeding and light/dark cycle conditions were used to perform transcriptome analysis. *Zmpste24*^{-/-} mice utilized for these experiments did not exhibit an overt cachectic phenotype which could confound further metabolic analysis. Labeling and hybridization reagents were prepared using master mixes at each step to minimize technical error. Biotin-labeled cRNA was produced from 2 μg total RNA using an Affymetrix 'one-way' labeling kit (catalog no. 900493). Total cRNA was then quantified using a Nano-Drop ND-1000 spectrophotometer and evaluated for quality after fragmentation on a 2100 Bioanalyzer. Following overnight hybridization at 45°C in an Affymetrix Model 640 GeneChip hybridization oven, the arrays were washed and stained using an Affymetrix 450 fluidics station as recommended by the manufacturer, and scanned on an Affymetrix Model 3000 scanner. After scanning, rawdata (Affymetrix Cel files) were obtained using Affymetrix GeneChip Operating Software (version 1.4). This software also provided summary reports by which array QA metrics were evaluated including average background, average signal and 3'/5' expression ratios for spike-in controls.

Analysis of gene expression

GenMAPP and Microsoft Excel software were used for the data analysis. GenMAPP (Gene MicroArray Pathway Profiler; <http://www.genmapp.org>) is a program for viewing and analyzing microarray data on microarray pathway profiles (MAPPs) representing biological pathways or any other functionally grouped genes (76). GenMAPP was used to construct and modify pathways as well as to provide access to annotations for genes of interest.

Histological analysis of tissues

Tissues were harvested and further fixed with 10% neutral-buffered formalin solution (Sigma) and left overnight at 4°C. After that, tissues were treated with 15% sucrose in PBS for 4 h, and then with 30% sucrose solution overnight. Tissue samples were embedded in Tissue-Tek OCT compound (Sakura Finetechnical Co. Ltd.) and stored at -70°C. Samples were then sectioned at 5 μm thickness with cryostat (CM3050 S, Leica). Cryosections were stained with PAS or Oil Red O to detect glycogen and triglycerides, respectively.

Statistical analysis

All experimental data are reported as mean and the error bars represent the standard error of the mean (SEM). Statistical analysis was performed by the non-parametric Student *t* test. Statistical analyses were made using the Prism program v. 4.0 (GraphPad software, Inc.).

SUPPLEMENTARY MATERIAL

Supplementary Material is available at HMG Online.

ACKNOWLEDGEMENTS

We thank Drs N. Mizushima, J. Hoeijmakers, M. Serrano, M.A. Blasco and R. Fernández for providing materials and reagents. We also thank Drs P. Boya, E. Knecht, A. Fueyo, P. Zuazua, A. Astudillo, A. Fernández and I. Santamaría for advice and M. Fernández, S. Alvarez, and M. S. Pitiot for excellent technical assistance.

Conflict of Interest statement. None declared.

FUNDING

This work was supported by grants from Ministerio de Educación y Ciencia-Spain, Fundación M. Botín, Fundación Lilly, Fundación La Caixa, and the European Union (Cancer Degradome-FP6 and FP7). The Instituto Universitario de Oncología is supported by Obra Social Cajastur-Asturias, Spain.

REFERENCES

- Kirkwood, T.B. (2005) Understanding the odd science of aging. *Cell*, **120**, 437–447.
- Massey, A.C., Kiffin, R. and Cuervo, A.M. (2006) Autophagic defects in aging: looking for an 'emergency exit'? *Cell Cycle*, **5**, 1292–1296.
- Muratani, M. and Tansey, W.P. (2003) How the ubiquitin–proteasome system controls transcription. *Nat. Rev. Mol. Cell. Biol.*, **4**, 192–201.
- Ciechanover, A. (2005) Proteolysis: from the lysosome to ubiquitin and the proteasome. *Nat. Rev. Mol. Cell. Biol.*, **6**, 79–87.
- Mizushima, N., Levine, B., Cuervo, A.M. and Klionsky, D.J. (2008) Autophagy fights disease through cellular self-digestion. *Nature*, **451**, 1069–1075.
- Marino, G. and Lopez-Otin, C. (2004) Autophagy: molecular mechanisms, physiological functions and relevance in human pathology. *Cell. Mol. Life Sci.*, **61**, 1439–1454.
- Terman, A., Gustafsson, B. and Brunk, U.T. (2007) Autophagy, organelles and ageing. *J. Pathol.*, **211**, 134–143.
- Cuervo, A.M. (2004) Autophagy: in sickness and in health. *Trends Cell Biol.*, **14**, 70–77.
- Cuervo, A.M., Bergamini, E., Brunk, U.T., Droge, W., Ffrench, M. and Terman, A. (2005) Autophagy and aging: the importance of maintaining 'clean' cells. *Autophagy*, **1**, 131–140.
- Del Roso, A., Vittorini, S., Cavallini, G., Donati, A., Gori, Z., Masini, M., Pollera, M. and Bergamini, E. (2003) Ageing-related changes in the in vivo function of rat liver macroautophagy and proteolysis. *Exp. Gerontol.*, **38**, 519–527.
- Hansen, M., Chandra, A., Mitic, L.L., Onken, B., Driscoll, M. and Kenyon, C. (2008) A role for autophagy in the extension of lifespan by dietary restriction in *C. elegans*. *PLoS Genet.*, **4**, e24.
- Simonsen, A., Cumming, R.C., Brech, A., Isakson, P., Schubert, D.R. and Finley, K.D. (2007) Promoting basal levels of autophagy in the nervous

- system enhances longevity and oxidant resistance in adult *Drosophila*. *Autophagy*, **4**, 151–175.
13. Vellai, T., Takacs-Vellai, K., Zhang, Y., Kovacs, A.L., Orosz, L. and Muller, F. (2003) Genetics: influence of TOR kinase on lifespan in *C. elegans*. *Nature*, **426**, 620.
 14. Ramirez, C.L., Cadinanos, J., Varela, I., Freije, J.M. and Lopez-Otin, C. (2007) Human progeroid syndromes, aging and cancer: new genetic and epigenetic insights into old questions. *Cell. Mol. Life. Sci.*, **64**, 155–170.
 15. Martin, G.M. and Oshima, J. (2000) Lessons from human progeroid syndromes. *Nature*, **408**, 263–266.
 16. Andressoo, J.O. and Hoeijmakers, J.H. (2005) Transcription-coupled repair and premature ageing. *Mutat. Res.*, **577**, 179–194.
 17. Navarro, C.L., Cau, P. and Levy, N. (2006) Molecular bases of progeroid syndromes. *Hum. Mol. Genet.*, **15** (Spec No. 2), R151–R161.
 18. Hennekam, R.C. (2006) Hutchinson-Gilford progeria syndrome: review of the phenotype. *Am. J. Med. Genet. A*, **140**, 2603–2624.
 19. Espada, J., Varela, I., Flores, I., Ugalde, A.P., Cadinanos, J., Pendas, A.M., Stewart, C.L., Tryggvason, K., Blasco, M.A., Freije, J.M. *et al.* (2008) Nuclear envelope defects cause stem cell dysfunction in premature-aging mice. *J. Cell Biol.*, **181**, 27–35.
 20. Varela, I., Cadinanos, J., Pendas, A.M., Gutierrez-Fernandez, A., Folgueras, A.R., Sanchez, L.M., Zhou, Z., Rodriguez, F.J., Stewart, C.L., Vega, J.A. *et al.* (2005) Accelerated ageing in mice deficient in Zmpste24 protease is linked to p53 signalling activation. *Nature*, **437**, 564–568.
 21. Sullivan, T., Escalante-Alcalde, D., Bhatt, H., Anver, M., Bhat, N., Nagashima, K., Stewart, C.L. and Burke, B. (1999) Loss of A-type lamin expression compromises nuclear envelope integrity leading to muscular dystrophy. *J. Cell Biol.*, **147**, 913–920.
 22. Pendas, A.M., Zhou, Z., Cadinanos, J., Freije, J.M., Wang, J., Hulthenby, K., Astudillo, A., Wernerson, A., Rodriguez, F., Tryggvason, K. *et al.* (2002) Defective prelamin A processing and muscular and adipocyte alterations in Zmpste24 metalloproteinase-deficient mice. *Nat. Genet.*, **31**, 94–99.
 23. Scaffidi, P. and Misteli, T. (2006) Lamin A-dependent nuclear defects in human aging. *Science*, **312**, 1059–1063.
 24. Haithcock, E., Dayani, Y., Neufeld, E., Zahand, A.J., Feinstein, N., Mattout, A., Gruenbaum, Y. and Liu, J. (2005) Age-related changes of nuclear architecture in *Caenorhabditis elegans*. *Proc. Natl Acad. Sci. USA*, **102**, 16690–16695.
 25. Hastay, P., Campisi, J., Hoeijmakers, J., van Steeg, H. and Vijg, J. (2003) Aging and genome maintenance: lessons from the mouse? *Science*, **299**, 1355–1359.
 26. Donati, A., Cavallini, G., Paradiso, C., Vittorini, S., Pollera, M., Gori, Z. and Bergamini, E. (2001) Age-related changes in the autophagic proteolysis of rat isolated liver cells: effects of antiaging dietary restrictions. *J. Gerontol. A Biol. Sci. Med. Sci.*, **56**, B375–B383.
 27. Donati, A., Cavallini, G., Carresi, C., Gori, Z., Parentini, I. and Bergamini, E. (2004) Anti-aging effects of anti-lipolytic drugs. *Exp. Gerontol.*, **39**, 1061–1067.
 28. Bergamini, E., Cavallini, G., Donati, A. and Gori, Z. (2004) The role of macroautophagy in the ageing process, anti-ageing intervention and age-associated diseases. *Int. J. Biochem. Cell Biol.*, **36**, 2392–2404.
 29. Kabeya, Y., Mizushima, N., Ueno, T., Yamamoto, A., Kirisako, T., Noda, T., Kominami, E., Ohsumi, Y. and Yoshimori, T. (2000) LC3, a mammalian homologue of yeast *Atg8p*, is localized in autophagosomal membranes after processing. *EMBO J.*, **19**, 5720–5728.
 30. Mizushima, N., Yamamoto, A., Matsui, M., Yoshimori, T. and Ohsumi, Y. (2004) In vivo analysis of autophagy in response to nutrient starvation using transgenic mice expressing a fluorescent autophagosome marker. *Mol. Biol. Cell.*, **15**, 1101–1111.
 31. Tanida, I., Minematsu-Ikeguchi, N., Ueno, T. and Kominami, E. (2005) Lysosomal turnover, but not a cellular level, of endogenous LC3 is a marker for autophagy. *Autophagy*, **1**, 84–91.
 32. Bjorkoy, G., Lamark, T., Brech, A., Outzen, H., Perander, M., Overvatn, A., Stenmark, H. and Johansen, T. (2005) p62/SQSTM1 forms protein aggregates degraded by autophagy and has a protective effect on huntingtin-induced cell death. *J. Cell Biol.*, **171**, 603–614.
 33. Abdenur, J.E., Brown, W.T., Friedman, S., Smith, M. and Lifshitz, F. (1997) Response to nutritional and growth hormone treatment in progeria. *Metabolism*, **46**, 851–856.
 34. Tian, M., Shinkura, R., Shinkura, N. and Alt, F.W. (2004) Growth retardation, early death, and DNA repair defects in mice deficient for the nucleotide excision repair enzyme XPF. *Mol. Cell Biol.*, **24**, 1200–1205.
 35. van der Pluijm, I., Garinis, G.A., Brandt, R.M., Gorgels, T.G., Wijnhoven, S.W., Diderich, K.E., de Wit, J., Mitchell, J.R., van Oostrom, C., Beems, R. *et al.* (2006) Impaired genome maintenance suppresses the growth hormone–insulin-like growth factor 1 axis in mice with Cockayne syndrome. *PLoS Biol.*, **5**, e2.
 36. Lum, J.J., DeBerardinis, R.J. and Thompson, C.B. (2005) Autophagy in metazoans: cell survival in the land of plenty. *Nat. Rev. Mol. Cell Biol.*, **6**, 439–448.
 37. Ravikumar, B., Vacher, C., Berger, Z., Davies, J.E., Luo, S., Oroz, L.G., Scaravilli, F., Easton, D.F., Duden, R., O’Kane, C.J. *et al.* (2004) Inhibition of mTOR induces autophagy and reduces toxicity of polyglutamine expansions in fly and mouse models of Huntington disease. *Nat. Genet.*, **36**, 585–595.
 38. Inoki, K., Zhu, T. and Guan, K.L. (2003) TSC2 mediates cellular energy response to control cell growth and survival. *Cell*, **115**, 577–590.
 39. Brugarolas, J., Lei, K., Hurley, R.L., Manning, B.D., Reiling, J.H., Hafen, E., Witters, L.A., Ellisen, L.W. and Kaelin, W.G., Jr (2004) Regulation of mTOR function in response to hypoxia by REDD1 and the TSC1/TSC2 tumor suppressor complex. *Genes Dev.*, **18**, 2893–2904.
 40. Pullen, N. and Thomas, G. (1997) The modular phosphorylation and activation of p70s6 k. *FEBS Lett.*, **410**, 78–82.
 41. Arsham, A.M. and Neufeld, T.P. (2006) Thinking globally and acting locally with TOR. *Curr. Opin. Cell Biol.*, **18**, 589–597.
 42. Hardie, D.G. (2004) The AMP-activated protein kinase pathway—new players upstream and downstream. *J. Cell Sci.*, **117**, 5479–5487.
 43. Alessi, D.R., Andjelkovic, M., Caudwell, B., Cron, P., Morrice, N., Cohen, P. and Hemmings, B.A. (1996) Mechanism of activation of protein kinase B by insulin and IGF-1. *EMBO J.*, **15**, 6541–6551.
 44. Manning, B.D., Tee, A.R., Logsdon, M.N., Blenis, J. and Cantley, L.C. (2002) Identification of the tuberous sclerosis complex-2 tumor suppressor gene product tuberlin as a target of the phosphoinositide 3-kinase/akt pathway. *Mol. Cell.*, **10**, 151–162.
 45. Shaw, R.J., Kosmatka, M., Bardeesy, N., Hurley, R.L., Witters, L.A., DePinho, R.A. and Cantley, L.C. (2004) The tumor suppressor LKB1 kinase directly activates AMP-activated kinase and regulates apoptosis in response to energy stress. *Proc Natl Acad. Sci. USA*, **101**, 3329–3335.
 46. Shaw, R.J., Lamia, K.A., Vasquez, D., Koo, S.H., Bardeesy, N., Depinho, R.A., Montminy, M. and Cantley, L.C. (2005) The kinase LKB1 mediates glucose homeostasis in liver and therapeutic effects of metformin. *Science*, **310**, 1642–1646.
 47. Feng, Z., Zhang, H., Levine, A.J. and Jin, S. (2005) The coordinate regulation of the p53 and mTOR pathways in cells. *Proc. Natl Acad. Sci. USA*, **102**, 8204–8209.
 48. Crighton, D., Wilkinson, S., O’Prey, J., Syed, N., Smith, P., Harrison, P.R., Gasco, M., Garrone, O., Crook, T. and Ryan, K.M. (2006) DRAM, a p53-induced modulator of autophagy, is critical for apoptosis. *Cell*, **126**, 121–134.
 49. Towler, M.C. and Hardie, D.G. (2007) AMP-activated protein kinase in metabolic control and insulin signaling. *Circ. Res.*, **100**, 328–341.
 50. Kahn, B.B., Alquier, T., Carling, D. and Hardie, D.G. (2005) AMP-activated protein kinase: ancient energy gauge provides clues to modern understanding of metabolism. *Cell Metab.*, **1**, 15–25.
 51. Long, Y.C. and Zierath, J.R. (2006) AMP-activated protein kinase signaling in metabolic regulation. *J. Clin. Invest.*, **116**, 1776–1783.
 52. Seoane, J., Gomez-Foix, A.M., O’Doherty, R.M., Gomez-Ara, C., Newgard, C.B. and Guinovart, J.J. (1996) Glucose 6-phosphate produced by glucokinase, but not hexokinase I, promotes the activation of hepatic glycogen synthase. *J. Biol. Chem.*, **271**, 23756–23760.
 53. Ferrer, J.C., Favre, C., Gomis, R.R., Fernandez-Novell, J.M., Garcia-Rocha, M., de la Iglesia, N., Cid, E. and Guinovart, J.J. (2003) Control of glycogen deposition. *FEBS Lett.*, **546**, 127–132.
 54. Yoon, J.C., Puigserver, P., Chen, G., Donovan, J., Wu, Z., Rhee, J., Adelmant, G., Stafford, J., Kahn, C.R., Granner, D.K. *et al.* (2001) Control of hepatic gluconeogenesis through the transcriptional coactivator PGC-1. *Nature*, **413**, 131–138.
 55. Gerhart-Hines, Z., Rodgers, J.T., Bare, O., Lerin, C., Kim, S.H., Mostoslavsky, R., Alt, F.W., Wu, Z. and Puigserver, P. (2007) Metabolic control of muscle mitochondrial function and fatty acid oxidation through SIRT1/PGC-1alpha. *EMBO J.*, **26**, 1913–1923.
 56. Wende, A.R., Huss, J.M., Schaeffer, P.J., Giguere, V. and Kelly, D.P. (2005) PGC-1alpha coactivates PDK4 gene expression via the orphan nuclear receptor ERRalpha: a mechanism for transcriptional control of muscle glucose metabolism. *Mol. Cell Biol.*, **25**, 10684–10694.

57. Araki, M. and Motojima, K. (2006) Identification of ERRA α as a specific partner of PGC-1 α for the activation of PDK4 gene expression in muscle. *FEBS J.*, **273**, 1669–1680.
58. Sarbassov, D.D., Ali, S.M. and Sabatini, D.M. (2005) Growing roles for the mTOR pathway. *Curr. Opin. Cell. Biol.*, **17**, 596–603.
59. Bonawitz, N.D., Chatenay-Lapointe, M., Pan, Y. and Shadel, G.S. (2007) Reduced TOR signaling extends chronological life span via increased respiration and upregulation of mitochondrial gene expression. *Cell Metab.*, **5**, 265–277.
60. Narbonne, P. and Roy, R. (2006) Inhibition of germline proliferation during *C. elegans* dauer development requires PTEN, LKB1 and AMPK signalling. *Development*, **133**, 611–619.
61. Apfeld, J., O'Connor, G., McDonagh, T., DiStefano, P.S. and Curtis, R. (2004) The AMP-activated protein kinase AAK-2 links energy levels and insulin-like signals to lifespan in *C. elegans*. *Genes Dev.*, **18**, 3004–3009.
62. Curtis, R., Geesaman, B.J. and DiStefano, P.S. (2005) Ageing and metabolism: drug discovery opportunities. *Nat. Rev. Drug. Discov.*, **4**, 569–580.
63. Kenyon, C. (2005) The plasticity of aging: insights from long-lived mutants. *Cell*, **120**, 449–460.
64. Russell, S.J. and Kahn, C.R. (2007) Endocrine regulation of ageing. *Nat. Rev. Mol. Cell. Biol.*, **8**, 681–691.
65. De Sandre-Giovannoli, A., Bernard, R., Cau, P., Navarro, C., Amiel, J., Boccaccio, I., Lyonnet, S., Stewart, C.L., Munnich, A., Le Merrer, M. *et al.* (2003) Lamin A truncation in Hutchinson-Gilford progeria. *Science*, **300**, 2055.
66. Eriksson, M., Brown, W.T., Gordon, L.B., Glynn, M.W., Singer, J., Scott, L., Erdos, M.R., Robbins, C.M., Moses, T.Y., Berglund, P. *et al.* (2003) Recurrent de novo point mutations in lamin A cause Hutchinson-Gilford progeria syndrome. *Nature*, **423**, 293–298.
67. Dechat, T., Shimi, T., Adam, S.A., Rusinol, A.E., Andres, D.A., Spielmann, H.P., Sinensky, M.S. and Goldman, R.D. (2007) Alterations in mitosis and cell cycle progression caused by a mutant lamin A known to accelerate human aging. *Proc. Natl Acad. Sci. USA*, **104**, 4955–4960.
68. Cao, K., Capell, B.C., Erdos, M.R., Djabali, K. and Collins, F.S. (2007) A lamin A protein isoform overexpressed in Hutchinson-Gilford progeria syndrome interferes with mitosis in progeria and normal cells. *Proc. Natl Acad. Sci. USA*, **104**, 4949–4954.
69. van de Ven, M., Andressoo, J.O., Holcomb, V.B., von Lindern, M., Jong, W.M., Zeeuw, C.I., Suh, Y., Hasty, P., Hoeijmakers, J.H., van der Horst, G.T. *et al.* (2006) Adaptive stress response in segmental progeria resembles long-lived dwarfism and calorie restriction in mice. *PLoS Genet.*, **2**, e192.
70. Niedernhofer, L.J., Garinis, G.A., Raams, A., Lalai, A.S., Robinson, A.R., Appeldoorn, E., Odijk, H., Oostendorp, R., Ahmad, A., van Leeuwen, W. *et al.* (2006) A new progeroid syndrome reveals that genotoxic stress suppresses the somatotroph axis. *Nature*, **444**, 1038–1043.
71. Kuma, A., Hatano, M., Matsui, M., Yamamoto, A., Nakaya, H., Yoshimori, T., Ohsumi, Y., Tokuhiya, T. and Mizushima, N. (2004) The role of autophagy during the early neonatal starvation period. *Nature*, **432**, 1032–1036.
72. Baehrecke, E.H. (2005) Autophagy: dual roles in life and death? *Nat. Rev. Mol. Cell. Biol.*, **6**, 505–510.
73. Gozuacik, D. and Kimchi, A. (2007) Autophagy and cell death. *Curr. Top. Dev. Biol.*, **78**, 217–245.
74. Marino, G., Salvador-Montoliu, N., Fueyo, A., Knecht, E., Mizushima, N. and Lopez-Otin, C. (2007) Tissue-specific autophagy alterations and increased tumorigenesis in mice deficient in Atg4C/autophagin-3. *J. Biol. Chem.*, **282**, 18573–18583.
75. Livak, K.J. and Schmittgen, T.D. (2001) Analysis of relative gene expression data using real-time quantitative PCR and the 2^{(-Delta Delta C(T))} Method. *Methods*, **25**, 402–408.
76. Dahlquist, K.D., Salomonis, N., Vranizan, K., Lawlor, S.C. and Conklyn, B.R. (2002) GenMAPP, a new tool for viewing and analyzing microarray data on biological pathways. *Nat. Genet.*, **31**, 19–20.